Journal of Drug Delivery Science and Technology 121 (2026) 108302

Contents lists available at ScienceDirect

Journal of Drug Delivery Science and Technology

journal homepage: www.elsevier.com/locate/jddst

Research paper

Timolol maleate-loaded double Pickering emulsion for the treatment of glaucoma: development, characterization, and ocular biocompatibility

Aniely dos Reis Teixeira [a,1], Liandra Gracher-Teixeira [b,1], Tatiana La Banca Schreiner [b], Arantzazu Santamaria-Echart [b], Viviane Flores Xavier [a], Gisele Rodrigues da Silva [a,*], Maria-Filomena Barreiro [b,**]

[a] School of Pharmacy, Federal University of Ouro Preto, Ouro Preto, Minas Gerais, 35400-000, Brazil
[b] CIMO, LA SusTEC, Instituto Politécnico de Bragança, Campus de Santa Apolónia, Bragança, 5300-253, Portugal

ARTICLE INFO

Keywords:
Drug delivery systems
Double pickering emulsion
Chitosan
Hydroxypropyl methylcellulose
Timolol maleate
Glaucoma treatment

ABSTRACT

Glaucoma is a leading cause of irreversible blindness, associated with high intraocular pressure. Topical beta-adrenergic antagonists, such as timolol maleate (TM), are first-line therapies but often have limited effectiveness due to rapid precorneal clearance and low ocular absorption. To address these limitations, a TM-loaded water-in-oil-in-water (W/O/W) double Pickering emulsion (TM-loaded DPE) was developed to enhance corneal retention, sustain drug release, and enhance ocular bioavailability. The TM-loaded DPE consisted of a primary W/O emulsion prepared from TM solution and mineral oil, stabilized by soy lecithin, combined with an external aqueous phase containing chitosan-Hydroxypropyl methylcellulose (chitosan-HPMC) particles as Pickering stabilizers, to form a W/O/W emulsion. Chitosan-HPMC particles had a size of 1.02 ± 0.16 μm, a zeta potential of 36.20 ± 2.41 mV, and a contact angle of 78.47 ± 1.80°, making them suitable Pickering stabilizers. The TM encapsulation efficiency in the TM-loaded DPE was 96%, indicating the high loading capacity of the developed system. Confocal laser scanning microscopy revealed a mononuclear droplet morphology, and the system exhibited excellent macroscopic physical stability under refrigerated conditions (4 °C, 12 months), as corroborated by the creaming index test, despite slight signs of coalescence observed in microscopic analysis. Rheological testing confirmed a non-Newtonian and shear-thinning behavior. The formulation achieved approximately 84% TM release over 48 h, indicating sustained release. The Hen egg test chorioallantoic membrane (HET-CAM) assay indicated no irritation potential, confirming its safety. Overall, these results highlight TM-loaded DPE as a promising drug delivery system for glaucoma treatment, offering improved drug retention and enhanced ocular bioavailability.

1. Introduction

Glaucoma is a chronic disease characterized by optic nerve dysfunction resulting from the progressive death of retinal ganglion cells, frequently associated with elevated intraocular pressure [1]. According to the World Health Organization (WHO) [2], glaucoma constitutes a significant public health challenge, affecting approximately 76 million people worldwide, and representing the primary cause of irreversible vision loss [3].

Increased intraocular pressure (IOP) arises from a disruption in the equilibrium between the aqueous humor formation and drainage [4]. The primary drainage route through the trabecular meshwork and Schlemm's canal, while the secondary outflow occurs via the uveoscleral, uveo-vortex, and uveo-lymphatic pathways [5]. Glaucoma treatment primarily aims to reduce IOP through pharmacological agents that either decrease aqueous humor production or facilitate its outflow, and, when necessary, is combined with laser trabeculoplasty and surgical interventions [6].

Currently, the primary pharmacological categories employed to reduce IOP include prostaglandin analogs, beta-adrenergic blockers, carbonic anhydrase inhibitors, and alpha-adrenergic agonists [7]. These medications are predominantly administered as topical eye drops, a

* Corresponding author. Federal University of Ouro Preto (UFOP), Morro do Cruzeiro s/n, Bauxita, 35400-000, Ouro Preto, Brazil.
** Corresponding author. Instituto Politécnico de Bragança (IPB), Campus de Santa Apolónia 5300-253, Bragança, Portugal.
E-mail addresses: giselersilva@ufop.edu.br (G.R. da Silva), barreiro@ipb.pt (M.-F. Barreiro).
[1] These authors have contributed equally to this work and share first authorship.

https://doi.org/10.1016/j.jddst.2026.108302
Received 25 December 2025; Received in revised form 1 April 2026; Accepted 2 April 2026
Available online 3 April 2026

preferred route for their rapid, localized effect and user-friendly application. Despite their widespread use, conventional ophthalmic formulations exhibit limited bioavailability in ocular tissues because a significant fraction of the drug is rapidly removed from the ocular surface shortly after application [8].

Several ocular anatomical and physiological factors contribute to this rapid drug clearance. Barriers such as the blood-aqueous barrier and the corneal and conjunctival epithelia limit drug permeation. Moreover, continuous tear fluid turnover, blinking, and nasolacrimal drainage, together with protective reflexes, reduce drug residence time on the ocular surface, thereby limiting their absorption [9]. Additionally, drugs may bind to tear proteins or be metabolically degraded by enzymes in the tear film, further diminishing their effective ocular bioavailability [10,11]. Given these limitations, frequent administration is required, which can lead to side effects, reduced patient adherence, and, ultimately, progressive vision loss or blindness [12].

Due to the inherent limitations of conventional ophthalmic formulations, glaucoma management remains challenging, prompting extensive research into innovative drug delivery systems. These include liposomes, nanoparticles, niosomes, dendrimers, ocular inserts, and hydrogels formulated from natural and synthetic biocompatible polymers and incorporated with IOP-lowering agents [12]. Such advanced delivery platforms aim to improve drug bioavailability, streamline dosing schedules, and ultimately enhance patient compliance with therapy.

Extensive scientific literature reviews highlight numerous studies dedicated to developing advanced drug delivery systems for glaucoma management. For example, Klézlová et al. [13] reported on non-conventional ocular drug delivery systems for glaucoma treatment, emphasizing innovative biomaterials to overcome current therapeutic limitations. Similarly, Albarqi et al. [11] reviewed various chitosan-based nanocarrier systems that significantly enhance drug residence time on the ocular surface, improve corneal penetration, and increase the bioavailability of encapsulated therapeutics. Additionally, Kesav et al. [14] provided a comprehensive overview of sustained-release drug delivery platforms designed for glaucoma management, emphasizing their potential to offer more effective and patient-friendly treatment options. Although various drug delivery systems for glaucoma have been extensively studied, double Pickering emulsions (DPEs) have not been reported as vehicles for the incorporation and administration of anti-glaucoma agents. Furthermore, to the best of the author's knowledge, this is the first report of a DPE for ophthalmic drug delivery using chitosan-Hydroxypropyl methylcellulose (chitosan-HPMC) particles as stabilizers, an innovative and unexplored strategy to enhance ocular drug bioavailability while eliminating safety concerns associated with synthetic ingredients.

The development of Pickering emulsions, which are emulsions stabilized by particles (Pickering stabilizers) rather than traditional molecular surfactants, presents a promising strategy for new drug delivery systems. These particles form physical barriers that effectively inhibit droplet coalescence and phase separation, thereby enhancing emulsion stability [15–17]. Compared with conventional surfactant-stabilized emulsions, Pickering-stabilized systems exhibit superior stability due to the robust mechanical barrier provided by the interfacial solid particles [17]. Building upon this stabilization strategy, DPEs, particularly the W/O/W systems employed in this study, represent more complex architectures in which a primary W/O emulsion is dispersed in a continuous aqueous phase containing Pickering particles to stabilize the secondary emulsion [18].

In this study, DPE were developed and loaded with timolol maleate (TM-loaded DPE) to enable effective drug delivery to the anterior segment of the eye for glaucoma treatment. TM, a non-selective β-adrenergic receptor antagonist, reduces IOP by inhibiting aqueous humor production in the ciliary body. The primary W/O emulsion was prepared using an aqueous solution of TM as the dispersed phase, mineral oil as the continuous oil phase, and soy lecithin as the surfactant. This primary emulsion was subsequently dispersed into an external aqueous phase and stabilized with chitosan-HPMC composite particles, thereby forming TM-loaded DPE. The selection of these excipients was intentional, as all components have established use in ophthalmic formulations or have been extensively investigated for ocular drug delivery applications [10,11,19]. Moreover, the resulting W/O/W Pickering emulsion exhibited a multicompartmental structure that protected the hydrophilic TM and enabled its controlled release. The ability of Pickering emulsion systems to preserve the chemical integrity of the drug within the emulsion phases and to promote sustained drug delivery constitutes key features for the development of innovative, non-conventional pharmaceutical dosage forms [20–22].

After producing the TM-loaded DPE, various analytical methods were used to confirm its morphology and assess its physicochemical, rheological, and morphological properties. Additionally, the *in vitro* release profile of TM from the DPE was evaluated to demonstrate its controlled drug-delivery capability. Finally, the *ex vivo* biocompatibility of the TM-loaded DPE was assessed using the chorioallantoic membrane assay of hen eggs (HET-CAM). The hypothesis proposed that TM-loaded DPE could serve as a promising therapeutic alternative for glaucoma treatment by enhancing corneal retention, enabling sustained drug release, and improving ocular bioavailability.

2. Materials and methods

2.1. Materials

Chitosan (85/10/A1) with a degree of deacetylation of 84.6%, and a dynamic viscosity of 20 mPa s at 20 °C (1% w/v in 1% acetic acid), corresponding approximately to a viscosity-average molecular weight of ~210 kDa, was supplied by Biotechnologie und Logistik GmbH (Landsberg, Germany). HMPC (grade SFE-400) with a dynamic viscosity of 371 mPa s at 20 °C (2% w/v in water) was kindly provided by Shin-Etsu Chemical Co., Ltd. (Tokyo, Japan). The Alifar mineral oil (neat form) was obtained from Instituto Galénico S.A. (Sintra, Portugal). Acetic acid was acquired from Honeywell Fluka (Charlotte, NC, United States of America). Soy lecithin was provided by Santiveri (Barcelona, Spain). TM eye drops (Timoglau®) at 2.5 mg/mL were obtained from Edol (Oeiras, Portugal) and contained the following excipients: monosodium phosphate monohydrate, disodium phosphate dodecahydrate, 50% benzalkonium chloride solution, sodium chloride, water for injections, hydrochloric acid, or sodium hydroxide.

2.2. Preparation of the chitosan-HPMC particles

Particles were prepared using 2% (w/v) HPMC and 2% (w/v) chitosan solutions following an adapted procedure of Yu et al. [23]. Briefly, HPMC was dissolved in distilled water, and chitosan was dissolved in acidified water (0.3 mol/L acetic acid). The solutions were stirred continuously at room temperature for 12 h using a magnetic stirrer (Rslab-1C, RSLab, Heraklion, Greece) to ensure complete dissolution. Then, equal volumes of both solutions were combined (25 mL each), with the HPMC solution gradually added to the chitosan solution using a peristaltic pump (MS-CA Series, Ismatec, Glattbrugg, Switzerland) at a flow rate of 18 mL/min and a stirring rate of 400 rpm to promote particle formation. Following the process, the particle dispersion was transferred to a glass vial and maintained at room temperature. The particles were coded as chitosan-HPMC particles.

2.3. Preparation of the double Pickering emulsions

The preparation of the double emulsion comprised two steps. The first, the primary emulsion, was prepared at a 30/70 (v/v) W/O ratio using distilled water and mineral oil. For the TM-loaded sample, the aqueous phase of the primary emulsion was replaced with timolol maleate eye drop (2.5 mg/mL). Soy lecithin (4% w/v, oil-basis), used as the

surfactant, was dissolved in the mineral oil at 60 °C under stirring at 400 rpm (20 min), then cooled. Subsequently, the aqueous and oil phases were transferred into a graduated cylinder and homogenized using an Ultra-Turrax homogenizer (Unidrive X-1000-CAT-Scientific, Ballrechten-Dottingen, Germany) at 14,500 rpm for 8 min.

For the second step, a (W/O)/W ratio of 50/50 (v/v) was used, and chitosan-HPMC particles were introduced as Pickering stabilizers. The chitosan-HPMC particle suspension (2%, w/v) was added dropwise to the primary W/O emulsion using a peristaltic pump at a flow rate of 18 mL/min, while maintaining stirring at 400 rpm. The mixture was then homogenized with an Ultra-Turrax homogenizer at 5000 rpm for 3 min. The unloaded DPE was coded as E1, and the TM-loaded DPE was coded as E2.

The selected composition for the primary emulsion was established following an initial screening in which various W/O ratios (20/80, 30/70, and 40/60) and lecithin concentrations (2, 3, and 4% w/v) were evaluated. Lecithin was chosen as the surfactant based on comparative tests with other surfactants and surfactant combinations, including Span 80 and Tween 80. For the double emulsion, the best performing primary emulsions were combined with the particles' dispersion, acting as the external aqueous phase of the W/O/W emulsion, and the stability was checked to select the most promising formulation. A summary of the tested conditions and main conclusions is provided as Supplementary Material.

2.4. Characterization of the chitosan-HPMC particles

Chitosan-HPMC particles were characterized in terms of size, zeta potential, and wettability.

2.4.1. Zeta potential and size

The zeta potential and size (hydrodynamic volume) of the chitosan-HPMC particles were determined using an electrophoretic light scattering instrument (Zetasizer Ultra Blue, Malvern Instruments, Worcestershire, UK). Before analysis [24], the samples were diluted with deionized water as the dispersant medium to minimize multiple-scattering effects. Each sample was analyzed in triplicate.

2.4.2. Wettability

The wettability was assessed using a contact angle goniometer (Ramé-Hart Instrument Co., Model 210, USA) equipped with an integrated camera. For that, particle films were prepared by casting. For that [24], particle pellets were prepared by drying the chitosan-HPMC particle dispersion in an oven at 40 °C for 3 days, followed by compression using a hydraulic press (SPECAC Manual Hydraulic Press, UK) at 78 kN. The three-phase contact angle was determined by immersing the pellet in 30 mL of mineral oil and depositing a water droplet (20 μL) onto the pellet surface. Contact angle values (θ) were continuously monitored for 30 s following droplet deposition (20 μL, water), and the reported values correspond to the stabilized measurement at 5 s. The instrument's image analysis software (DROPimage Pro) automatically calculated the left and right angles using the Young-Laplace equation. All experiments were done in triplicate at room temperature using freshly prepared films, and results were expressed as mean ± standard deviation (SD).

2.5. Characterization of the TM-loaded DPE

The TM-loaded DPE was characterized with respect to droplet size, zeta potential, and pH; type and morphology (drop test and Confocal Laser Scanning Microscopy - CLSM); stability (optical microscopy monitoring and creaming index); rheological behavior; encapsulation efficiency; and ocular biocompatibility.

2.5.1. Encapsulation efficiency

TM encapsulation efficiency (EE) in the loaded DPE was determined using an indirect method adapted from Hemar et al. [25]. Briefly, 2 mL of freshly prepared TM-loaded DPE was centrifuged at 500×*g* for 20 min at 25 °C to separate the external aqueous phase. Subsequently, 0.1 mL of the supernatant was collected, diluted with 7.9 mL of ultrapure water, and centrifuged again at 7500×*g* for 30 min to remove any remaining particulate matter. The resulting solution was filtered through a 0.45 μm syringe filter and analyzed by UV-visible spectroscopy (V-730, Jasco Inc., Tokyo, Japan) at 294 nm. The concentration of non-encapsulated TM was determined using a validated UV spectrophotometric method at 306 nm. The method demonstrated selectivity, with UV spectra recorded between 200 and 400 nm showing no matrix interference. It exhibited linearity over the concentration range of 2.5-500 μg/mL ($y = 0.0067x + 0.3284$, $r^2 = 0.9987$), precision (relative standard deviation, RSD <4%) and accuracy, with recoveries ranging from 98% to 102%. The limit of detection (LOD) and limit of quantification (LOQ) were 1.62 μg/mL and 4.91 μg/mL, respectively. Encapsulation efficiency (%) was calculated based on Equation (1). All measurements were performed in triplicate, and results were reported as mean ± SD.

$$EE(\%) = \frac{Q\ total - Q\ free}{Q\ total} \times 100 \quad (1)$$

where *Q total* is the total amount of drug added to the formulation and *Q free* is the amount of non-encapsulated drug determined in the supernatant.

2.5.2. Droplet size analysis and zeta potential

The droplet size was measured using laser diffraction (Mastersizer 2000, Malvern Instruments, Worcestershire, UK). Measurements were performed in volume and number at room temperature using water as the dispersant phase [26]. Results were reported as Dv10, Dv50 and Dv90. Span index, which reflects the dispersion of the distribution, was determined according to Equation (2).

$$Span = \frac{(Dv90 - Dv10)}{Dv50} \quad (2)$$

where Dv10, Dv50, and Dv90 represent the droplet sizes below which 10%, 50%, and 90% of the total droplet volume distribution were found, respectively. Five consecutive measurements were acquired for each sample.

For the zeta potential determination, the procedure described for the particles in section 2.4.1 was followed.

2.5.3. pH determination

Emulsion pH was measured in triplicate using a calibrated pH meter (inoLab pH 720, WTW GmbH, Weilheim, Germany). Calibration was performed using standard buffer solutions at pH 4.0 and 7.0 before measurements. All pH readings were taken at room temperature (25 °C).

2.5.4. Emulsion type

The emulsion type was initially confirmed using the drop test. For that, a droplet of the emulsion was placed into 10 mL of purified water or mineral oil. A uniform dispersion in the aqueous phase indicates an external aqueous phase, whereas a dispersion in the oily phase corresponds to an external oily phase [27]. The test was performed on both the primary W/O emulsions and the W/O/W emulsions, including the optimized TM-loaded DPE.

2.5.5. Morphology - CLSM

For the TM-loaded DPE, high-resolution analysis of the interfacial microstructure was performed using CLSM on a Leica TCS-SP5 AOBS system (Leica Microsystems Inc., Heidelberg, Germany) [28]. The emulsion was stained with fluorescent dyes Nile red (oil phase) and Nile blue (stabilizer), each at 1% (w/v) in DMSO, mixed with the emulsion at a 1:10 ratio. Nile red and Nile blue were excited using an argon laser at wavelengths of 488 nm and 633 nm, respectively. This dual staining approach enabled separate visualization of the oil and particles to assess

the system's stabilization mechanism.

2.5.6. Emulsion stability

The macroscopic emulsion stability was evaluated by measuring the creaming index (CI) at two temperatures (4 and 25 °C) to identify the best storage conditions for the developed product [18]. The CI (expressed in %) was calculated using Equation (3).

$$CI\ (\%) = \frac{HS}{HT} x\ 100 \quad (3)$$

where HS represent height of the separated serum phase and HT the total height of the emulsion. The evaluation was conducted at predetermined intervals of 0, 7, 15, 30, 60, and 365 days.

This analysis was accompanied by optical microscopy (OM), which can help discern early signs of microscopic instability, using an Eclipse 50i microscope equipped with a Nikon imaging system (Nikon Instruments Inc., New York, USA). Sample preparation [18] involved placing an aliquot of the double Pickering emulsion onto a glass slide and gently covering it with a coverslip. Images were captured and saved using NIS-Elements Documentation software 5.01.

2.5.7. Rheological behavior

The rheological behavior was characterized using a Kinexus Lab + controlled stress rheometer (Netzsch, Selb, Germany). Measurements were performed using a parallel cone-plate geometry with a 40 mm-diameter upper plate and a 1 mm gap at 20 °C [24]. Viscosity was measured over a shear-rate range of 0.01 to 100 s^{-1} to evaluate flow behavior. To assess the viscoelastic properties, oscillatory tests were conducted. An amplitude sweep was performed at a fixed frequency of 1 Hz, varying shear strain from 0.01% to 100% to determine the linear viscoelastic region (LVR). The yield stress was identified at the crossover point where the storage modulus (G′) intersected the loss modulus (G″). Subsequently, frequency-sweep tests were conducted over 0.01 to 10 Hz at a constant strain of 0.5% (within the LVR) to further characterize the viscoelastic response.

2.6. Evaluation of the DPE performance

2.6.1. In vitro drug release of TM from DPE

The drug release profile was determined using the Franz vertical diffusion cell (Hanson Research, Phoenix RDS, USA). The donor and receptor compartments were separated by a dialysis membrane (MW 12,000-14,000 Da), into which 100 μL of the sample was added, corresponding to 0.036 mg of TM. The receptor medium consisted of 20 mL of simulated tear fluid maintained under constant agitation at 37 °C for up to 48 h. Samples (500 μL) were collected at predetermined time intervals of 0.5, 1, 3, 6, 12, 24, and 48 h, with the medium being replaced after each collection (500 μL). The assay was conducted under sink conditions. The drug quantification was performed with a plate reader (Tecan Infinite Pro 200, Switzerland) at 306 nm, following the method described in section 2.5.1. The release profile was evaluated as the cumulative percentage of TM delivered from DPE in the medium (n = 5). Higuchi, zero order, first order, and Korsmeyer-Peppas mathematical models were applied to evaluate the kinetic profile of the drug [29].

2.6.2. Hen egg test chorioallantoic membrane (HET-CAM) irritation test

Fertilized hen eggs were obtained from a poultry farm (Alimentos Rivelli, MG, Brazil) and incubated in an automatic GP® incubator (SP, Brazil) at 37 ± 0.5 °C and 40 ± 4% relative humidity for 10 days. During incubation, eggs were rotated daily and placed horizontally for several minutes each time to ensure proper embryo positioning. On day 10, each egg was opened by gently cracking the underside against the edge of a plastic Petri dish, exposing the CAM. A 300 μL volume of each test sample was applied directly to the CAM surface (n = 5 per sample). After 20 s of exposure, the CAM was carefully rinsed with 5 mL of physiological saline solution to remove any residual test substance. The CAM was then observed at 0.5-, 2-, and 5-min post-application for physiological reactions, which were graded based on their time of appearance according to the criteria outlined in Table 1. Observed effects included hemorrhage (diffuse blood release from vessels and/or capillaries), vascular lysis (disintegration of blood vessels), and coagulation (protein denaturation both intra- and extravascular), following the definitions of Luepke [30]. Final classification of the formulations' irritability potential, as determined by the HET-CAM assay, is summarized in Table 2. The tested samples included: (1) sodium hydroxide 0.1 mol/L (positive control); (2) TM eye drops (2.5 mg/mL); (3) unloaded DPE; and (4) TM-loaded DPE. Eggs prior to sample application (time 0) were used as negative controls.

2.7. Statistical analysis

For droplet size measurements, a paired Student's t-test was performed using SPSS Statistics software version 27.0 (IBM Corp., Armonk, NY, USA) to compare day 0 and day 30 values within the same samples (n = 5). Results were expressed as mean ± SD of five consecutive technical replicates. Differences were considered statistically significant when $p < 0.05$.

3. Results

3.1. Characterization of the chitosan-HPMC particles

The obtained particles had a hydrodynamic diameter of 1.02 ± 0.16 μm, measured by dynamic light scattering, and a zeta potential of +36.20 ± 2.41 mV. The zeta potential is an important parameter that influences physicochemical stability; a higher absolute zeta potential (>30 mV) indicates a stable dispersion system [31]. Using ~1 μm particles is expected to yield Pickering emulsions with a coarse morphology and behavior governed by particle concentration and wettability. Moreover, a three-phase contact angle of 78.47 ± 1.80° (Fig. 1) was observed, confirming the particle's preferential affinity for the aqueous phase and suitability as Pickering stabilizers for O/W emulsions, making them suitable for incorporation into the external aqueous phase during the preparation of the W/O/W emulsions, promoting O/W interfacial adsorption and Pickering stabilization.

For the produced chitosan-HPMC particles, a three-phase contact angle (θ) of 78.47 ± 1.80° (Fig. 1) was measured in mineral oil, confirming their preferential affinity for the aqueous phase and suitability as Pickering stabilizers for O/W emulsions, making them ideal candidates for incorporation into the external aqueous phase during the preparation of the W/O/W emulsions, promoting O/W interfacial adsorption and Pickering stabilization.

3.2. Characterization of the TM-loaded DPE

3.2.1. Encapsulation efficiency

The encapsulation efficiency was evaluated after incorporating the TM solution (2.5 mg/mL), yielding 96%. The high encapsulation efficiency confirmed the successful incorporation of the drug into the internal aqueous phase, likely facilitated by its hydrophilic properties. The results are similar to the 93% encapsulation percentage reported by Tang et al. [32] in a double emulsion using chitosan and HPMC.

Table 1
Events grading in the chorioallantoic membrane of embryonated chicken eggs.

Event	Time		
	≤30 s	30 s < t ≤ 2 min	2 min < t ≤ 5 min
Hyperemia	5	3	1
Hemorrhage	7	5	3
Coagulation/opacity	9	7	5

Table 2
Irritation score classification range.

Range (grading of lesions)	Classification
0.0 - 0.9	Non-irritating
1.0 - 4.9	Mildly irritating
5.0 - 8.9	Moderately irritating
9.0 - 21	Severely irritating

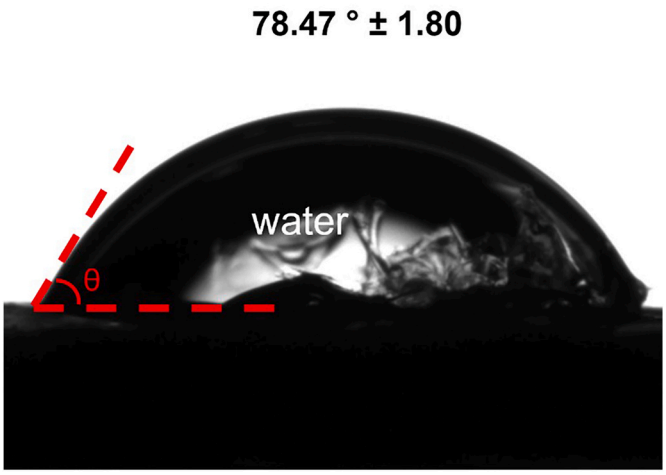

Fig. 1. Contact angle (θ) of chitosan-HPMC particles.

3.2.2. Droplet size, zeta potential, and pH

Fig. 2 shows the distribution of droplet sizes in volume and number of unloaded DEP (E1) and TM-loaded DPE (E2), both freshly prepared (time zero) and after 30 days of storage at 4 °C and 25 °C. While the number-based distribution was unimodal, the volume-based distribution showed a bimodal pattern with two distinct droplet populations spanning a wide size range (Fig. 2), as evidenced by high polydispersity, indicated by span values of 2.38-4.90 (Table 3). Such distributions are characteristic of double-emulsion systems prepared by mechanical emulsification, in which multiple droplet populations are inherently part of the system's structure [33]. To better reflect this polydispersity, the sizes are reported as Dv10, Dv50 and Dv90 in Table 3. Although statistically significant differences ($p < 0.05$) were detected between day 0 and day 30 for most parameters, particularly at 25 °C, the observed variations were minimal in absolute terms, suggesting that the formulation remained practically stable over the storage period. At 4 °C, E1 showed minimal variation (<3%) across all measured parameters, whereas E2 showed a small but statistically significant change in Dv50 (1.6%) and a pronounced increase in Dv90. At 25 °C, E2 showed the most pronounced temporal variation, with a statistically significant decrease in Dv90 from day 0 to day 30. These results predict an enhanced emulsion stability at 4 °C and a beneficial effect of TM incorporation.

Regarding the zeta potential, which was determined right after production, values of +68.65 ± 1.12 mV and +62.53 ± 0.85 mV were observed for E1 and E2, respectively. These values indicate a slight reduction in zeta potential after drug incorporation, without any indication of compromised stability, as both systems fall within the range associated with high stability.

The pH of the emulsion was measured to assess its compatibility with the ocular region, as it is essential that the emulsion not alter the pH of this region. The measurement revealed that the emulsion had a pH of 4.8.

3.2.3. Emulsion type and morphology

Drop test analysis confirmed the successful formation of the double-emulsion structure. The primary W/O emulsion droplets aggregated immediately upon introduction into the aqueous medium and remained uniformly dispersed in the oil phase, confirming their water-in-oil nature. The final double Pickering emulsion (W/O/W) droplets dispersed uniformly in the aqueous medium but aggregated in the oil phase, thereby validating the water-continuous external-phase characteristic of the W/O/W system. The visual inspection is shown in Fig. 3.

CLSM analysis, performed only on the E2 sample, confirmed the multiple W/O/W emulsion structure and indicated a predominant mononuclear morphology, as shown in the images of Fig. 4. Moreover, the emulsion exhibits a coarse morphology with many droplets ≥10 μm. Compared with laser diffraction measurements, CLSM provides a more realistic visualization of droplets because it is a direct observation. Moreover, laser diffraction tends to underestimate size due to sample dilution and its higher sensitivity to smaller droplets. In Fig. 4A, large green, mostly ring-like structures correspond to the oil phase, composed of mineral oil. They encapsulate an internal droplet, marked in red in Fig. 4B, indicating their aqueous nature and compatibility with the TM solution. Additionally, it is suggested that the distinct bright red coloration observed at the interfaces between the two phases corresponds to soy lecithin, the surfactant responsible for stabilizing the primary W/O emulsion. Surrounding this primary emulsion, chitosan-HPMC particles were visible as bright red dots at the interface between the oil phase and the external aqueous phase, which can promote bridging effects, thus reinforcing emulsion stability (Fig. 4C).

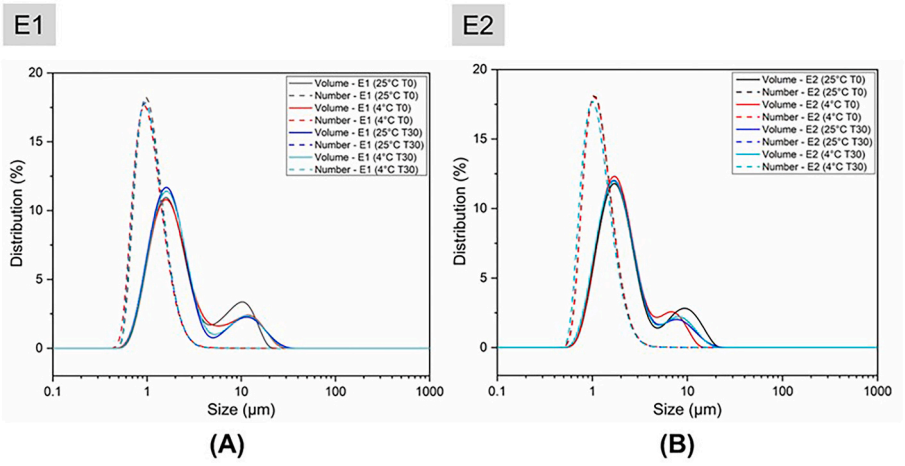

Fig. 2. Droplet size distribution of E1 (unloaded DPE) and E2 (TM-loaded DPE), both freshly prepared (time zero – T0) and after 30 days (T30) of storage at 4 °C and 25 °C.

Table 3
Droplet diameter (Dv10, Dv50 and Dv90) (μm), and Span values of unloaded DPE (E1) and TM-loaded DPE (E2) at time zero and after 30 days of storage at 4 °C and 25 °C.

Samples	Time (days)	Temperature							
		4 °C				25 °C			
		Dv10 (μm)	Dv50 (μm)	Dv90 (μm)	Span	Dv10 (μm)	Dv50 (μm)	Dv90 (μm)	Span
E1	**0**	1.00 ± 0.002	1.88 ± 0.003	9.84 ± 0.052	4.70 ± 0.030	1.03 ± 0.003	1.91 ± 0.008	9.60 ± 0.056	4.50 ± 0.030
	30	1.01 ± 0.000	1.84 ± 0.003*	9.81 ± 0.061	4.78 ± 0.080*	1.00 ± 0.000*	1.80 ± 0.000*	9.83 ± 0.017*	4.90 ± 0.080*
E2	**0**	1.08 ± 0.003	1.89 ± 0.004	5.59 ± 0.054	2.38 ± 0.002	1.09 ± 0.004	1.95 ± 0.005	8.62 ± 0.107	3.86 ± 0.040
	30	1.04 ± 0.000*	1.86 ± 0.001*	6.41 ± 0.014*	2.88 ± 0.007*	1.04 ± 0.000*	1.86 ± 0.000*	6.00 ± 0.003*	2.66 ± 0.080*

Values represent mean ± SD of five consecutive replicates. *$p < 0.05$ compared to day 0 (paired Student's t-test).

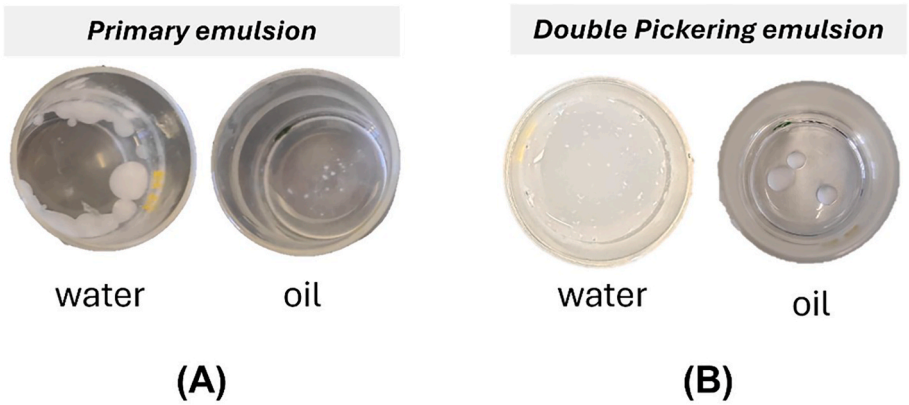

Fig. 3. Drop test to confirm the emulsion type. (A) Primary emulsion droplets aggregate in water and exhibit uniform dispersion in oil. (B) DPE droplets show uniform dispersion in water and aggregation in oil.

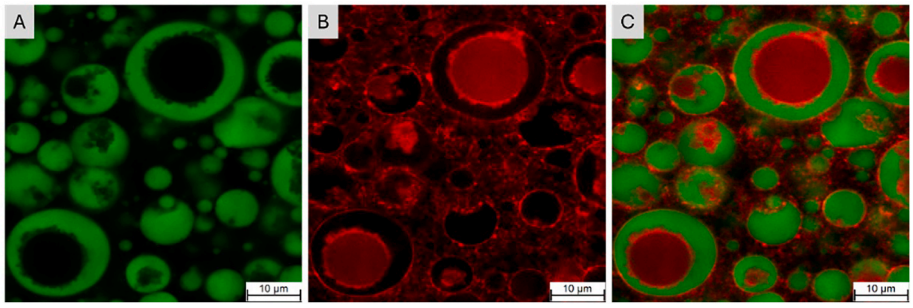

Fig. 4. Confocal Laser Scanning Microscopy (CLSM) images showing the W/O/W structure of the TM-loaded DPE. Large green droplets represented the oil phase composed of mineral oil (A), Red large droplets represent the water phase (B), and the combination of them (C). Scale bar: 10 μm. Magnification: 40 × . Zoomed-in view 4.4 X. (For interpretation of the references to color in this figure legend, the reader is referred to the Web version of this article.)

3.2.4. *Emulsion stability*

Optical microscopy analysis of both E1 and E2 samples over time at 4 °C and 25 °C is shown in Figs. 5 and 6, respectively, covering a period of 365 days. For the E1 sample (Fig. 5), only the 0- and 365-day images are shown. For the E2 sample (Fig. 6), a detailed time-course analysis was performed at 0, 7, 15, 30, 60, and 365 days. Both formulations showed temperature-dependent stability under the tested conditions. At 4 °C, the formulation retained its spherical morphology throughout storage. For E2, the TM-loaded DPE stored at 25 °C (Fig. 6B) maintained its structural integrity for up to 60 days, with a gradual increase in droplet size becoming evident at 365 days. Similarly, E1 showed comparable behavior, with increased droplet size observed after 365 days at 25 °C (Fig. 5B) compared to the initial timepoint (Fig. 5A).

The creaming index of both E1 and E2 was evaluated over 365 days at 4 °C and 25 °C (Figs. 7 and 8). Both formulations maintained their macroscopic characteristics during storage at 4 °C, with a creaming index of 0, indicating stability. In contrast, both samples (E1 and E2) showed increasing creaming indices over time at 25 °C, with phase separation occurring after 60 days for the E2 sample and after 365 days for the E1 sample (Table 4), indicating formulation instability at higher temperatures.

3.2.5. *Rheological behavior*

Both E1 and E2 exhibited a non-Newtonian and shear-thinning behavior, where their apparent viscosity gradually decreased with increasing shear rate (0 to 100 s^{-1}). This phenomenon was attributed to the breakdown of the emulsion's internal microstructure under increasing shear stress (Fig. 9A).

The strain sweep tests (Fig. 9B) revealed similar viscoelastic behavior for both formulations. Both emulsions initially showed stable storage (G') and loss (G'') moduli within their linear viscoelastic regions (LVR), with G'' consistently higher than G', characteristic of liquid-like behavior. Within the LVR, both formulations exhibited comparable viscoelastic properties, suggesting that the incorporation of TM did not

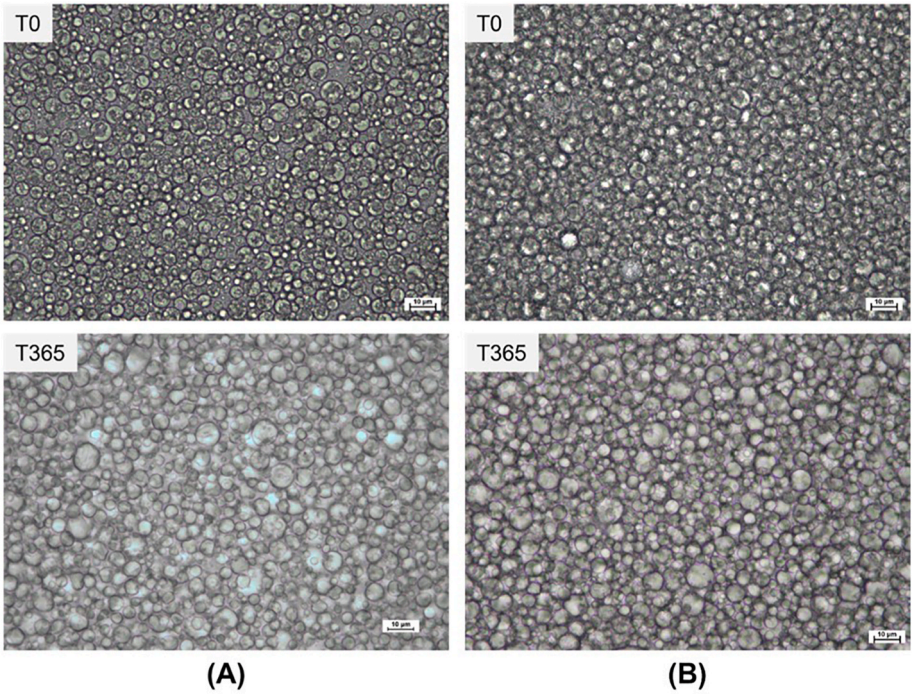

Fig. 5. Optical micrographs of E1 (unloaded DPE), on the first day prepared, and after 365 days during storage at (A) 4 °C and (B) 25 °C. Scale bar: 10 μm (400X magnification).

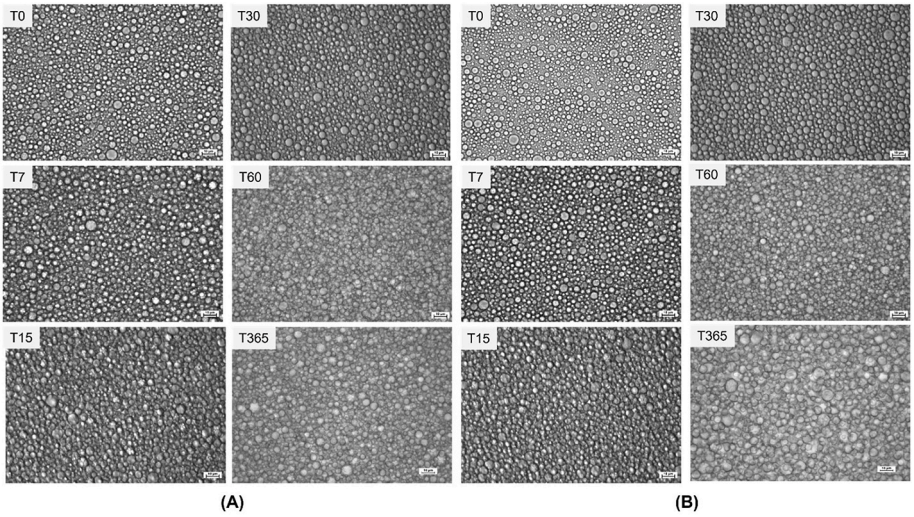

Fig. 6. Optical micrographs of E2 (TM-loaded DPE) during storage at (A) 4 °C and (B) 25 °C over 365 days (0, 7, 15, 30, 60, and 365 days). Scale bar: 10 μm (400 × magnification).

significantly alter the system's mechanical behavior.

Dynamic oscillatory measurements (Fig. 9C) further confirmed that both emulsions were predominantly liquid-viscous, as the loss modulus (G″) consistently exceeded the storage modulus (G′) across the tested frequency range. This indicated a dominant viscous component in their overall rheological response.

3.3. Evaluation of the DPE performance

3.3.1. In vitro drug release

The *in vitro* release profile of TM from the developed DPE was evaluated under simulated ocular physiological conditions, and the obtained results are shown in Fig. 10. Within the first 4 h, approximately 48% of the drug was released from the DPE, indicating an initial burst release. Subsequently, TM was released gradually, with about 84% of the drug detected in the medium after 48 h, indicating a sustained release period.

The *in vitro* TM release data from the DPE were fitted to the Higuchi, zero-order, first-order, and Korsmeyer–Peppas mathematical models, and the corresponding correlation coefficients (R^2) were presented in Table 5. Among the models evaluated, the Korsmeyer–Peppas model provided the best fit to the experimental data, as indicated by the highest R^2 value when compared with the other models, suggesting that it more accurately describes the TM release kinetics from the DPE. Moreover, in this model, the diffusional exponent (n) provides insight into the dominant release mechanism. For spherical systems, n values ≤ 0.43 indicate Fickian diffusion-controlled release. In the present study, the n value was 0.39, lower than 0.43, indicates that TM release from the DPE

Fig. 7. Macroscopic images of E1 (unloaded DPE) during storage at (A) 4 °C and (B) 25 °C over 365 days (0, 7, 15, 30, 60, and 365 days).

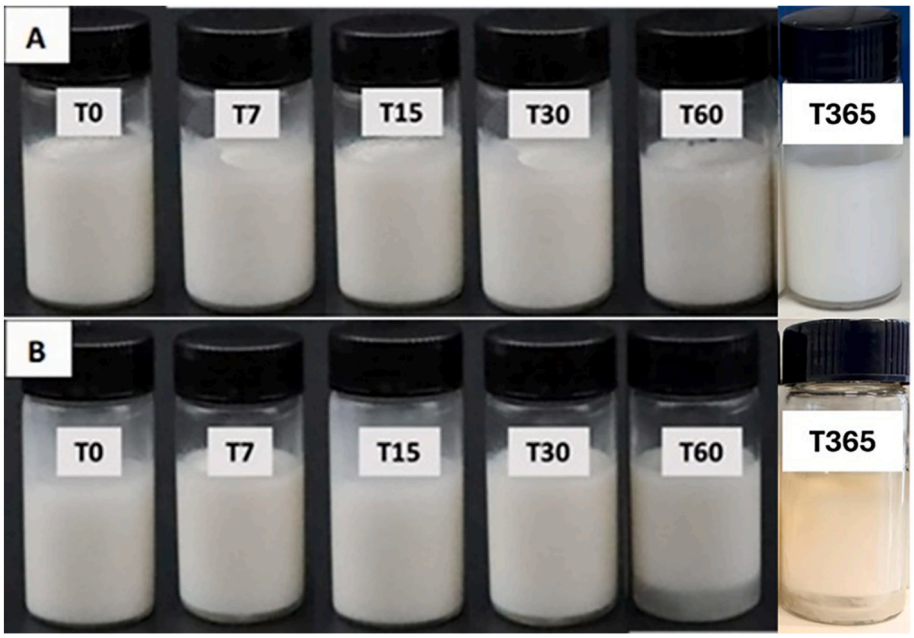

Fig. 8. Macroscopic images of E2 (TM-loaded DPE) during storage at (A) 4 °C and (B) 25 °C over 60 days (0, 7, 15, 30, 60 and 365 days).

Table 4
Creaming index of E1 (unloaded DPE) and E2 (TM-loaded DPE) storage at 4 and 25 °C for 0, 7, 15, 30, 60 and 365 days.

Time (days)	Creaming Index (%)			
	4 °C		25 °C	
	E1	E2	E1	E2
T0	0	0	0	0
T7	0	0	0	0
T15	0	0	0	0
T30	0	0	0	0
T60	0	0	0	20
T365	0	0	15	20

is predominantly governed by Fickian diffusion through the DPE system.

3.3.2. *HET-CAM*

The toxicity assays performed on embryonated chicken eggs demonstrated that the positive control (0.1 mol/L NaOH) induced intense hemorrhage and coagulation across all replicates within 30 s, causing severe irritation of the CAM vascular system, thereby confirming the validity of the model (Fig. 11). In contrast, treatment with TM eye drops (2.5 mg/mL) showed no signs of irritation. Similarly, the unloaded DPE and TM-loaded DPE did not cause hyperemia, hemorrhage, or coagulation and were therefore classified as non-irritating based on the irritation score.

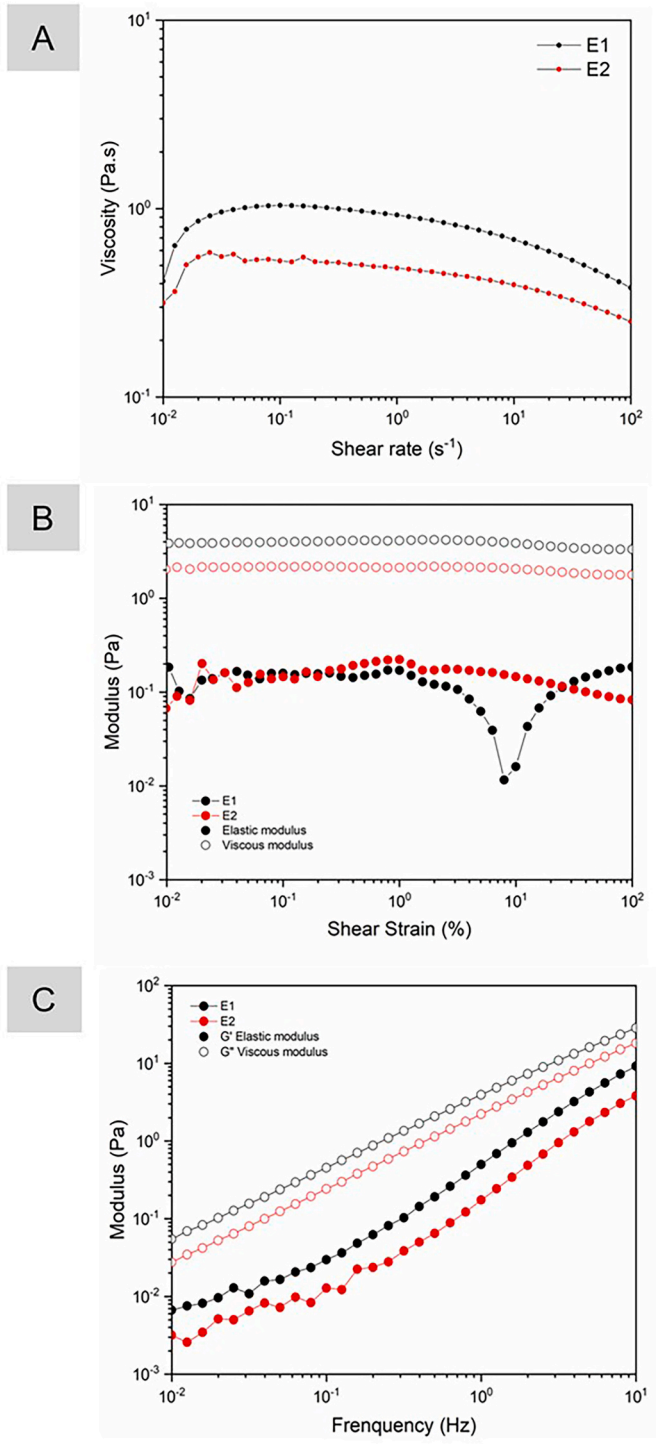

Fig. 9. Rheological characterization of E1 (unloaded DPE) and E2 (TM-loaded DPE).

4. Discussion

The TM-loaded DPE was prepared through a two-step emulsification process. The initial step involved forming a primary W/O emulsion, stabilized by soy lecithin. Soy lecithin is a natural amphiphilic surfactant composed primarily of phospholipids such as phosphatidylcholine (PC), phosphatidylethanolamine (PE), phosphatidylinositol (PI), and phosphatidic acid (PA). In particular, the relatively lower contents of PC and PE contribute to enhanced stabilization of W/O emulsions. Moreover, these components induce a negative spontaneous curvature at the

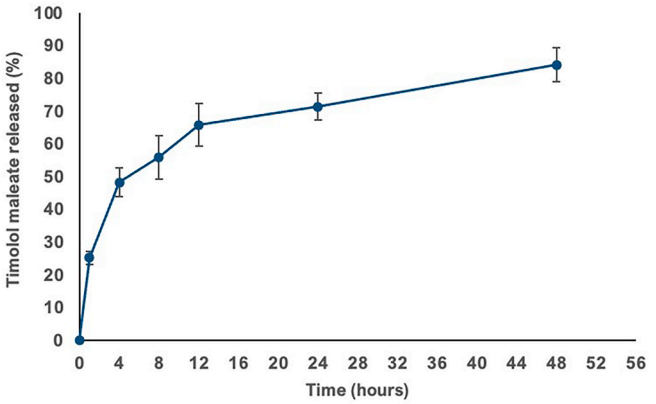

Fig. 10. Cumulative percentage of TM released from DPE in simulated tear fluid. Data were presented as mean ± SD (n = 5).

Table 5
Correlation coefficients obtained from the Higuchi, zero-order, first-order, and Korsmeyer–Peppas mathematical models used to describe the TM release kinetic profile from the DPE. The diffusional exponent (*n*) calculated using the Korsmeyer-Peppas model is also presented.

Correlation coefficient (R^2)			
Higuchi	Zero-order	First-order	Korsmeyer–Peppas
0.8939	0.7345	0.5678	0.9757 (n = 0.39)

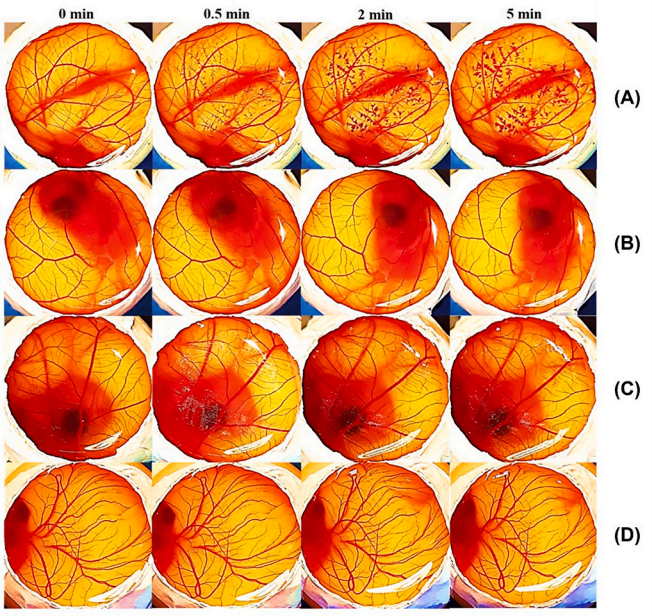

Fig. 11. HET-CAM assay: CAM exposed to 0.1 mol/L NaOH solution (positive control) (A), which caused hemorrhage; TM from eye drops at 2.5 mg/mL (B); E1, unloaded DPE (C); and E2, TM-loaded DPE (D), which did not induce irritation. (n = 5 for each sample).

phospholipid bilayer interface [34,35], thereby ensuring the stability of the W/O system with TM confined within the inner aqueous phase.

Subsequently, the primary emulsion was supplemented with an external aqueous phase containing chitosan-HPMC particles, thereby forming a W/O/W Pickering system. The stability of this final system relies on the Pickering mechanism provided by the composite particles. Chitosan-HPMC particles had a size of 1.02 ± 0.16 μm, a zeta potential

of +36.20 ± 2.41 mV, and a three-phase contact angle of 78.47 ± 1.80°, making them suitable Pickering stabilizers for O/W interfaces [36]. Wettability is a crucial factor for effective emulsion stabilization, as reported by Ribeiro et al. [28]. This inherent hydrophilicity arises from the protonated amino groups in chitosan and the hydrophilic hydroxypropyl groups in HPMC [37–39]. Furthermore, the hydrophobic methylcellulose segments of HPMC interact with the oil phase; whereas its hydrophilic groups extend into the external aqueous phase, establishing a robust Pickering barrier that prevents droplet contact [40].

The morphology of the W/O and W/O/W was first validated by drop test analysis and further corroborated by CLSM. The drop test analysis provided a simple yet effective confirmation of the emulsion type at each stage of the formulation. For the primary W/O emulsion, the immediate aggregation in water and uniform dispersion in oil confirmed its W/O nature, validating the successful formation of the first emulsification step [27]. This behavior results from the hydrophobic continuous phase of the W/O emulsion, which naturally resists mixing with water but readily disperses in oil media. Conversely, the final double Pickering emulsion exhibited the opposite behavior: uniform dispersion in water and aggregation in oil, confirming the characteristic water-continuous external phase of W/O/W systems [33].

CLSM images confirmed a predominant mononuclear morphology in the W/O/W Pickering emulsion, consistent with the reported advantages reported by Wang et al. [41]. Their well-defined structure with a single water core enables better control of material transport between phases, making them particularly valuable for applications in biological and biomedical research. Also, as described by Guo et al. [42] and Yuan et al. [43], it can contribute to structural uniformity by minimizing the complexity of internal droplet arrangements.

CLSM images revealed that the droplets existed as discrete entities, with no notable interactions or aggregation, confirming the effectiveness of the dual stabilization mechanism: lecithin at the inner W/O interface and chitosan-HPMC particles at the external O/W interface. The tightly adsorbed layer formed by chitosan-HPMC particles via Pickering stabilization, together with the system's viscous behavior, provided a robust mechanical barrier that prevented droplet contact and maintained structural integrity throughout the system. This physical separation mechanism aligns with findings from Du et al. [44] and Tenorio-Garcia et al. [45], who demonstrated, e.g., that increased viscosity in Pickering emulsions played a crucial role in physically separating droplets and preventing coalescence.

The unloaded and TM-loaded DPE systems exhibited high positive zeta potentials (+68.65 ± 1.12 and +62.53 ± 0.85 mV, respectively), thereby providing colloidal stability by inducing strong electrostatic repulsion between droplets and preventing coalescence [39]. The results obtained by Li et al. [46] also showed that chitosan-particle-stabilized emulsions at higher concentrations exhibit increased Pickering emulsion stability. In their study, coalescence and phase separation were observed at lower concentrations (0.025% and 0.05%) due to insufficient particle concentration to stabilize the high-oil fraction. Despite the differences in particle composition, both studies confirm the fundamental requirement of adequate particle concentration for proper interfacial coverage in Pickering emulsion systems. The conditions used in this work, a 2% composite particle (1:1, chitosan-HPMC ratio) dispersion, were sufficient to achieve droplet coverage and enhance stability through additional particle bridging, as observed in the CLMS images.

The TM-loaded DPE was characterized by a droplet population with a Dv50 of ~2 μm and a Dv90 of ~6 μm, as measured by laser diffraction, with span values (2.38-4.90) indicating broader size distributions and the coexistence of droplet populations across different size ranges [47]. CLMS images clearly showed droplets >10 μm, providing direct, in situ visualization of the emulsion. The size of the nano/micro entities is often described as crucial for minimizing irritation of the anterior segment of the eye, as irritation can decrease the drug's residence time on the ocular surface and, consequently, limit its absorption [48], even though deformable liquid droplets can spread, flatten, and reorganize on the ocular surface, surpassing this effect. For this reason, conducting performance tests that assess drug release and irritation upon application is of high importance.

Droplet size is often associated with emulsion stability by reducing the incidence of coalescence and creaming, two standard mechanisms that drive destabilization [33]. The overall stability of highly concentrated emulsions, colloidal systems with a higher dispersed-phase volume, is significantly dependent on inter-droplet forces (disjoining pressure) and the tenacity of the interfacial film [31]. These findings are corroborated by those reported by Gracher-Teixeira et al. [49] in a study of double emulsions, in which droplet size directly affected emulsion stability, with smaller, more homogeneous droplets correlating with enhanced stability and reduced phase separation.

Despite the observed droplet polydispersity, the DPE systems remained stable for 365 days of storage, particularly for the TM-loaded DPE at 4 °C, as confirmed by a zero-creaming index. The mechanical strength of the chitosan-HPMC particle barrier at the oil-water interface is compromised by thermal energy, leading to decreased emulsion stability and increased coalescence at 25 °C [50]. The stability at 4 °C can be attributed to reduced thermal motion, which preserves the structural integrity of the chitosan-HPMC particle barrier, consistent with reported temperature-dependent behavior of chitosan-based Pickering systems, minimized droplet collisions, and slowed diffusion kinetics [43,50]. To highlight that both formulations remained stable for 365 days at 4 °C with minimal changes in droplet size. Therefore, refrigerated storage at 4 °C is essential for maintaining the long-term physicochemical stability of the developed system, corroborating results from similar systems [51] and ensuring their suitability for pharmaceutical applications.

Rheological analyses showed that both formulations exhibited pseudoplastic (shear-thinning) behavior, typical of structured emulsions and beneficial for ocular delivery systems. Incorporating TM reduced viscosity and viscoelastic moduli relative to the unloaded formulation, suggesting a less organized internal network, likely due to interactions between TM and the chitosan-HPMC matrix or interfacial components. Both systems exhibited viscoelastic liquid behavior ($G'' > G'$), confirming their predominantly viscous nature rather than gel-like behavior. The viscosity of the TM-loaded DPE is a key formulation characteristic, as it prolongs residence time in the anterior segment of the eye, helping overcome the common challenge of low bioavailability in ophthalmic drug delivery. Moreover, this extended ocular retention is further enhanced by the mucoadhesive properties of chitosan and HPMC in the formulation. In fact, HPMC is a water-soluble, biocompatible, first-generation mucoadhesive polymer widely used in ophthalmic preparations for its lubricating effects and ability to mimic the natural tear film [52]. Chitosan, a cationic polysaccharide, exhibits mucoadhesion primarily through electrostatic interactions between its positively charged amino groups and the negatively charged sialic acid residues of mucin in the ocular mucus. This ionic binding significantly prolongs residence time on the ocular surface [53]. Therefore, both polymers synergistically enhance the retention of TM-loaded DPE and improve TM bioavailability in the eye.

The DPE exhibited a two-phase release profile for TM. In the initial phase (4 h), the release rate increased sharply, indicating a rapid burst release. This initial burst was likely driven by the presence of very small droplets with a larger surface area, which rapidly swelled and released the drug. This phase was followed by a sustained release lasting up to 48 h. The controlled release during this period was probably influenced by the chitosan-HPMC nanoparticles, which formed a viscous physical barrier that slowed the diffusion of TM through the system. Therefore, the TM release mechanism was fitted to the Korsmeyer–Peppas model, indicating that drug release is governed by water penetration into the polymer matrix followed by diffusion of the drug. These findings align with those of Zang et al. [54], who demonstrated that Pickering emulsions stabilized by chitosan hydrochloride-carboxymethyl starch nanoparticles served as an effective diffusion barrier, thereby regulating the

lixiviation of tea polyphenols in the medium. The prolonged TM release profile from the DPE represents a promising strategy for glaucoma management by enhancing the drug's ocular bioavailability, reducing administration frequency, and thereby improving patient adherence to therapy.

Finally, *ex vivo* biocompatibility was assessed using the HET-CAM assay, which closely resembles conjunctival tissue in its rich vascular network and responsiveness to inflammatory and irritant challenges. Both tissues are highly vascularized mucous membranes, making the CAM an effective model for studying how materials interact with the eye's surface. Because of these analogous properties, the CAM has become a preferred alternative for biocompatibility testing, particularly in assessing the irritation and toxicity risks of ophthalmic formulations [55,56]. In the present study, the *ex vivo* biocompatibility of TM-loaded DPE was evaluated by direct application to the CAM. The membrane showed no signs of vascular irritation, such as hemorrhage, tissue degradation, or coagulation, suggesting that TM-loaded DPE is unlikely to cause similar adverse effects in conjunctival tissue upon direct contact. This biocompatibility is crucial for preventing rapid clearance of the formulation from the eye's anterior segment, thereby enhancing its therapeutic effectiveness in glaucoma treatment.

Overall, these findings, together with the high TM encapsulation efficiency (96%), highlight these systems as a promising drug delivery platform for glaucoma treatment, with the potential to improve ocular retention and enhance drug bioavailability.

From a future perspective, using an animal model of glaucoma is the next step in this research to strengthen the scientific evidence for TM-loaded DPE.

5. Conclusions

In this study, an unloaded and TM-loaded DPE was developed by first preparing a W/O emulsion using mineral oil as the hydrophobic phase and soy lecithin as the surfactant, followed by stabilization with chitosan-HPMC particles to form the DPE. CLSM provided a detailed visualization of the TM-loaded DPE, revealing well-defined droplet interfaces coated with soy lecithin and chitosan-HPMC particles. The formulation exhibited remarkable stability for 12 months at 4 °C, with no signs of coalescence or creaming, highlighting the need for refrigerated storage. This stability was mainly attributed to the high positive surface charge (zeta potential $> +60$ mV) arising from protonated chitosan at the droplet interfaces, which promoted strong electrostatic repulsion, and to the viscous interfacial layer conferred by the chitosan-HPMC particles through Pickering stabilization, which restricted droplet mobility and prevented coalescence. Moreover, the DPE demonstrated controlled and sustained release of TM over 48 h. Importantly, the TM-loaded DPE elicited no irritation in the hen's egg CAM assay, confirming its ocular biocompatibility. Collectively, these physicochemical and biological properties position TM-loaded DPE as a promising therapeutic approach for glaucoma, extending ocular residence time, improving drug bioavailability, and ultimately enhancing patient compliance. Future steps including *in vivo* and pharmacokinetic studies would provide a deepener overview about the clinical translation and ocular retention potential of the formulation.

CRediT authorship contribution statement

Aniely dos Reis Teixeira: Conceptualization, Investigation, Methodology, Validation, Writing – original draft. **Liandra Gracher-Teixeira:** Conceptualization, Investigation, Methodology, Validation, Writing – original draft. **Tatiana La Banca Schreiner:** Investigation, Methodology, Writing – original draft. **Arantzazu Santamaria-Echart:** Investigation, Validation, Writing – review & editing. **Viviane Flores Xavier:** Investigation, Methodology. **Gisele Rodrigues da Silva:** Conceptualization, Funding acquisition, Supervision, Writing – review & editing. **Maria-Filomena Barreiro:** Conceptualization, Funding acquisition, Resources, Supervision, Writing – review & editing.

Declaration of competing interest

The authors declare that they have no known competing financial interests or personal relationships that could have appeared to influence the work reported in this paper.

Acknowledgements

This research was supported by the National Council for Scientific and Technological Development (CNPq, Brazil) under grants 402092/2022-8, 309559/2021-9, and 304105/2024-4, and by the Minas Gerais State Research Support Foundation (FAPEMIG, Brazil) through grant APQ-00182-22. We also acknowledge the UFOP Multiuser Laboratory 1 of the Graduate Program in Pharmaceutical Sciences (CiPharma) for the analyses performed. Foundation for Science and Technology (FCT, Portugal) for financial support via national funds FCT/MCTES (PIDDAC) to CIMO UID/00690/2025 (10.54499/UID/00690/2025) and UID/PRR/00690/2025 (10.54499/UID/PRR/00690/2025); and SusTEC, LA/P/0007/2020 (DOI: 10.54499/LA/P/0007/2020). FCT through the institutional scientific employment program contract of A. Santamaria-Echart and Liandra Gracher-Teixeira PhD research grant 2020.08803.BD (DOI: 10.54499/2020.08803.BD) is acknowledged.

Appendix A. Supplementary data

Supplementary data to this article can be found online at https://doi.org/10.1016/j.jddst.2026.108302.

Data availability

Data will be made available on request.

References

[1] H. Jayaram, M. Kolko, D.S. Friedman, G. Gazzard, Glaucoma: now and beyond, Lancet 402 (2023) 1788–1801, https://doi.org/10.1016/S0140-6736(23)01289-8.
[2] World Health Organization, World Report on Vision, World Health Organization, Geneva, 2019. https://iris.who.int/bitstream/handle/10665/328717/9789241516570-eng.pdf. (Accessed 23 October 2025), 2019.
[3] J.D. Steinmetz, R.R.A. Bourne, S. Resnikoff, T. Ackland, J.B. Braithwaite, M. Bron, A. Cicinelli, A. Das, J. Jonas, J. Keeffe, J.H. Kempen, J. Leasher, et al., Causes of blindness and vision impairment in 2020 and trends over 30 years, Lancet Global Health 9 (2021) e144–e160, https://doi.org/10.1016/S2214-109X(20)30489-7.
[4] R.N. Weinreb, T. Aung, F.A. Medeiros, The pathophysiology and treatment of glaucoma, JAMA 311 (2014) 1901–1911, https://doi.org/10.1001/jama.2014.3192.
[5] A. Narayanaswamy, S. Baskaran, R. Zheng, A. Lavanya, R. Sakata, T. Tun, C. Y. Cheng, T. Aung, Aqueous outflow channels and its lymphatic association: a review, Surv. Ophthalmol. 67 (2022) 659–674, https://doi.org/10.1016/j.survophthal.2021.10.004.
[6] A.P. Mai, M. Kim, J. Park, S. Lee, H. Kim, New treatments for glaucoma, Curr. Opin. Ophthalmol. 36 (2025) 135–139, https://doi.org/10.1097/ICU.0000000000001110.
[7] R.E. Reddy, V. Kumar, S. Singh, P. Yadav, A. Sharma, Review of the synthesis of timolol maleate and brimonidine tartrate, Org. Process Res. Dev. 29 (2025) 3–14, https://doi.org/10.1021/acs.oprd.4c00280.
[8] E.M. del Amo, Topical ophthalmic administration, Front. Drug Deliv. 2 (2022) 954771, https://doi.org/10.3389/fddev.2022.954771.
[9] S. Li, L. Chen, Y. Fu, Nanotechnology-based ocular drug delivery systems, J. Nanobiotechnol. 21 (2023) 232, https://doi.org/10.1186/s12951-023-01992-2.
[10] T. Ahmed, M. Khan, S. Ali, R. Hussain, N. Iqbal, Polysaccharide polymers for glaucoma treatment, Eur. J. Ophthalmol. 34 (2024) 338–356, https://doi.org/10.1177/11206721231178057.
[11] H.A. Albarqi, A. Garg, M.Z. Ahmad, A.A. Alqahtani, I.A. Walbi, J. Ahmad, Recent progress in chitosan-based nanomedicine for its ocular application in glaucoma, Pharmaceutics 15 (2023) 681, https://doi.org/10.3390/pharmaceutics15020681.
[12] O.L. Lanier, M.G. Manfre, C. Bailey, Z. Liu, Z. Sparks, S. Kulkarni, A, Chauhan, Review of approaches for increasing ophthalmic bioavailability for eye drop formulations, AAPS PharmSciTech 22 (2021) 107, https://doi.org/10.1208/s12249-021-01977-0.
[13] A. Klézlová, P. Bulíř, A. Klápšťová, M. Netuková, K. Šenková, J. Horáková, P. Studený, Novel biomaterials in glaucoma treatment, Biomedicines 12 (2024) 813, https://doi.org/10.3390/biomedicines12040813.

[14] N.P. Kesav, M.K. Ertel, L.K. Seibold, M.Y. Kahook, Sustained-release drug delivery systems for the treatment of glaucoma, Int. J. Ophthalmol. 14 (2021) 148–159, https://doi.org/10.18240/ijo.2021.01.21.
[15] I. Dammak, P.J.A. Sobral, Formulation optimization of lecithin-enhanced Pickering emulsions stabilized by chitosan nanoparticles for hesperidin encapsulation, J. Food Eng. 229 (2018) 2–11, https://doi.org/10.1016/j.jfoodeng.2017.11.001.
[16] R.D. Bachu, P. Chowdhury, Z.H.F. Al-Saedi, P.K. Karla, S.H.S. Boddu, Ocular drug delivery barriers: role of nanocarriers in the treatment of anterior segment ocular diseases, Pharmaceutics 10 (2018) 28, https://doi.org/10.3390/pharmaceutics10010028.
[17] J. Paredes-Toledo, J. Herrera, J. Morales, P. Robert, J. Gómez-Estaca, B. Giménez, Pickering double emulsions stabilized with chitin nanocrystals and myristic acid-functionalized silica nanoparticles for curcumin and chlorogenic acid co-delivery, Pharmaceutics 17 (2025) 521, https://doi.org/10.3390/pharmaceutics17040521.
[18] L.G. Teixeira, S. Rezende, Â. Fernandes, I.P. Fernandes, L. Barros, J.C.M. Barreira, F.V. Leimann, I.C.F.R. Ferreira, M.F. Barreiro, Water-in-oil-in-water double emulsions as protective carriers for Sambucus nigra L. coloring systems, Molecules 27 (2022) 552, https://doi.org/10.3390/molecules27020552.
[19] F.A. Maulvi, D.T. Desai, P. Kalaiselvan, S. Dumpati, R. Kuppusamy, S. Masoudi, D. O. Shah, M.D.P. Willcox, Lipid-based eye drop formulations for the management of evaporative dry eyes, Contact Lens Anterior Eye 47 (2024) 102154, https://doi.org/10.1016/j.clae.2024.102154.
[20] Z. Huang, R.V. Moiseev, S.S. Melides, W. Bae, I. Jurewicz, V.V. Khutoryanskiy, J. L. Keddie, Pickering emulsions stabilised with oligoglycine-functionalised nanodiamond as a model system for ocular drug delivery applications, Soft Matter 19 (2023) 5513–5526, https://doi.org/10.1039/d3sm00495c.
[21] Z. Li, D. Yu, Formulation and characterization of pH-responsive Pickering emulsions stabilized by soy protein isolate/nicotinamide mononucleotide complexes for controlled drug release, Ind. Crops Prod. 203 (2023) 117158, https://doi.org/10.1016/j.indcrop.2023.117158.
[22] Z. Li, D. Yu, Controlled ibuprofen release from Pickering emulsions stabilized by pH-responsive cellulose-based nanofibrils, Int. J. Biol. Macromol. 242 (2023) 124942, https://doi.org/10.1016/j.ijbiomac.2023.124942.
[23] X.H. Yu, F.Z. Zhou, Y.K. Xi, X.N. Huang, S.W. Yin, X.Q. Yang, Ethyl cellulose–chitosan complex particle-stabilized W/O Pickering emulsions as recyclable biocatalytic microreactors, Colloids Surf. A Physicochem. Eng. Asp. 639 (2022) 128375, https://doi.org/10.1016/j.colsurfa.2022.128375.
[24] B.M. Oliveira, G. Colucci, T.B. Schreiner, G. Preegel, L.L. Silva, A. Santamaria-Echart, M.F. Barreiro, Lignin–quercetin hybrid colloidal particles as sustainable Pickering emulsifiers: a bio-based and functional approach, Molecules 31 (2026) 889, https://doi.org/10.3390/molecules31050889.
[25] Y. Hemar, L.J. Cheng, C.M. Oliver, L. Sanguansri, M. Augustin, Encapsulation of resveratrol using water-in-oil-in-water double emulsions, Food Biophys. 5 (2010) 120–127, https://doi.org/10.1007/s11483-010-9152-5.
[26] G. Colucci, A. Ribeiro, M.B. Figueiredo, J. Charmillot, A. Santamaria-Echart, A. E. Rodrigues, M.F. Barreiro, Lignin from aldehyde-assisted fractionation can provide light-colored pickering emulsions through colloidal particles formed using alkaline antisolvent, Int. J. Biol. Macromol. 302 (2025) 140534, https://doi.org/10.1016/j.ijbiomac.2025.140534.
[27] S.C. Silva, T. Almeida, G. Colucci, A. Santamaria-Echart, Y.A. Manrique, M.M. Dias, L. Barros, A. Fernandes, E. Colla, M.F. Barreiro, Spirulina (*Arthrospira platensis*) protein-rich extract as a natural emulsifier for oil-in-water emulsions: optimization through a sequential experimental design strategy, Colloids Surf. A Physicochem. Eng. Asp. 648 (2022) 129264, https://doi.org/10.1016/j.colsurfa.2022.129264.
[28] A. Ribeiro, Y.A. Manrique, J.C.B. Lopes, M.M. Dias, M.F. Barreiro, Development of water-in-oil pickering emulsions from sodium oleate surface-modified nano-hydroxyapatite, Surf. Interfaces 29 (2022) 101759, https://doi.org/10.1016/j.surfin.2022.101759.
[29] L. Popa, M.V. Ghica, R. Popescu, T. Irimia, C.E. Dinu-Pîrvu, Development and optimization of chitosan–hydroxypropyl methylcellulose in situ gelling systems for ophthalmic delivery of bupivacaine hydrochloride, Processes 9 (2021) 1694, https://doi.org/10.3390/pr9101694.
[30] P. Luepke, Hen's egg chorioallantoic membrane test for irritation potential, Food Chem. Toxicol. 23 (1985) 287–291, https://doi.org/10.1016/0278-6915(85)90030-4.
[31] R. Foudazi, S. Qavi, I. Masalova, A.Ya Malkin, Physical chemistry of highly concentrated emulsions, Adv. Colloid Interface Sci. 220 (2015) 78–91, https://doi.org/10.1016/j.cis.2015.03.002.
[32] K. Tang, S. Pei, H. Xing, Y. Chen, M. Lin, Y. Liu, L. Lin, Y. Zhu, Long-term stable water-in-oil-in-water emulsion for effective protection and sustained release of lysine-calcium using chitosan and hydroxypropyl methylcellulose, Int. J. Biol. Macromol. 282 (2024) 137098, https://doi.org/10.1016/j.ijbiomac.2024.137098.
[33] D.J. McClements, Food Emulsions: Principles, Practices and Techniques, third ed., Taylor & Francis, Boca Raton, 2016.
[34] M. Wang, W. Yan, Y. Zhou, L. Fan, Y. Liu, J. Li, Progress in the application of lecithins in water-in-oil emulsions, Trends Food Sci. Technol. 118 (2021) 388–398, https://doi.org/10.1016/j.tifs.2021.10.019.
[35] M. Balcaen, J. Steyls, A. Schoeppe, V. Nelis, P. Van der Meeren, Phosphatidylcholine-depleted lecithin: a clean-label low-HLB emulsifier to replace PGPR in W/O and W/O/W emulsions, J. Colloid Interface Sci. 581 (2021) 836–846, https://doi.org/10.1016/j.jcis.2020.07.149.
[36] Y.K. Kwok, Wettability on different surfaces, in: 21st Century Surface Science: a Handbook, IntechOpen, London, 2020, https://doi.org/10.5772/intechopen.92885.
[37] X. Qiu, D. Yan, L. Xu, Y. Wang, Y. Mao, C. Yang, Y. Li, Y. Sun, Topical delivery performance of Pickering emulsions stabilized by differently charged spirulina protein isolate/chitosan composite particles, Int. J. Pharm. 671 (2025) 125284, https://doi.org/10.1016/j.ijpharm.2025.125284.
[38] V. Martínez, M.I. Maguregui, R.M. Jiménez, R.M. Alonso, Determination of the pKa values of β-blockers by automated potentiometric titrations, J. Pharm. Biomed. Anal. 23 (2000) 459–468, https://doi.org/10.1016/S0731-7085(00)00324-1.
[39] S.N. Shareef, B.P. Narasaiah, W. Madhuri, K. Vagdevi, Ramnarayan, Carbon quantum dots-doped chitosan/HPMC nanocomposites and their functional, structural, morphological, dielectric and tensile properties, E3S Web Conf. 430 (2023) 01149, https://doi.org/10.1051/e3sconf/202343001149.
[40] R.T. Shimada, M.S. Fonseca, D.F.S. Petri, The role of hydroxypropyl methylcellulose structural parameters on the stability of emulsions containing Spirulina biomass, Colloids Surf. A Physicochem. Eng. Asp. 529 (2017) 137–145, https://doi.org/10.1016/j.colsurfa.2017.06.001.
[41] J. Wang, S. Hahn, E. Amstad, N. Vogel, Tailored double emulsions made simple, Adv. Mater. 34 (2022) 2107338, https://doi.org/10.1002/adma.202107338.
[42] L. Guo, M. Cao, X. Chen, L. Zhang, X. Zhang, L. Zou, W. Liu, One-step fabrication of microfluidic W/O/W droplets as fat-reduced high internal phase emulsions: microstructure, stability and 3D printing performance, Food Hydrocoll. 150 (2024) 109742, https://doi.org/10.1016/j.foodhyd.2024.109742.
[43] S. Yuan, H. Wang, Q. Du, J. Fang, Mechanistic insights into heat-induced demulsification of oil/water emulsions driven by surfactant type, Colloids Surf. A Physicochem. Eng. Asp. 728 (2026) 138489, https://doi.org/10.1016/j.colsurfa.2025.138489.
[44] L. Du, Z. Meng, Engineering surfactant-free pickering double emulsion gels with different structures as low-calorie fat analogues: tunable oral perception, inhibiting lipid digestion, and potent co-delivery for lycopene and epigallocatechin gallate, Food Chem. 463 (2025) 141378, https://doi.org/10.1016/j.foodchem.2024.141378.
[45] E. Tenorio-Garcia, A. Araiza-Calahorra, M. Rappolt, E. Simone, A. Sarkar, Pickering water-in-oil emulsions stabilized solely by fat crystals, Adv. Mater. Interfaces. 10 (2023) 2300190, https://doi.org/10.1002/admi.202300190.
[46] Y. Li, M. Chen, Y. Ding, Y. Li, M. Guo, Y. Zhang, A Pickering emulsion stabilized by chitosan-g-poly(N-vinylcaprolactam) microgels: interface formation, stability and stimuli-responsiveness, Carbohydr. Polym. 332 (2024) 121948, https://doi.org/10.1016/j.carbpol.2024.121948.
[47] L.D. Daza, M. Umaña, V.S. Eim, Effect of the addition of chachafruto flour on the stability of oil-in-water emulsions and the physicochemical properties of spray-drying microcapsules, Food Chem. 462 (2025) 141025, https://doi.org/10.1016/j.foodchem.2024.141025.
[48] T.F. Vandamme, Microemulsions as ocular drug delivery systems: recent developments and future challenges, Prog. Retin. Eye Res. 21 (2002) 15–34, https://doi.org/10.1016/S1350-9462(01)00017-9.
[49] L. Gracher-Teixeira, S.C.S. Pituco, G. Colucci, A. Santamaria-Echart, A.M. Peres, M. M. Dias, M.F. Barreiro, Developing high-coloring natural systems using double emulsions with Daucus carota L. extract to meet high-performance requirements, Foods 13 (2024) 4147, https://doi.org/10.3390/foods13244147.
[50] P. Rattanaburi, N. Charoenrat, T. Pongtharangkul, M. Suphantharika, J. Wongkongkatep, Hydroxypropyl methylcellulose enhances the stability of O/W Pickering emulsions stabilized with chitosan and whole cells of Lactococcus lactis IO-1, Food Res. Int. 116 (2019) 559–565, https://doi.org/10.1016/j.foodres.2018.08.074.
[51] H. Yang, Z. Su, X. Meng, X. Zhang, J.F. Kennedy, B. Liu, Fabrication and characterization of Pickering emulsions stabilized by soy protein isolate–chitosan nanoparticles, Carbohydr. Polym. 247 (2020) 116712, https://doi.org/10.1016/j.carbpol.2020.116712.
[52] S.N. Sanap, A.C. Bisen, A. Kedar, K.S. Yadav, A. Krishna, A. Akhir, S. Chopra, M. N. Mugale, R.S. Bhatta, Chitosan/HPMC-based mucoadhesive film co-loaded with fluconazole and ofloxacin for management of polymicrobial keratitis, Int. J. Biol. Macromol. 222 (2022) 2785–2795, https://doi.org/10.1016/j.ijbiomac.2022.10.058.
[53] M. Silva, R. Calado, J. Marto, A. Bettencourt, A. Almeida, L. Gonçalves, Chitosan nanoparticles as a mucoadhesive drug delivery system for ocular administration, Mar. Drugs 15 (2017) 370, https://doi.org/10.3390/md15120370.
[54] L. Zhang, J.K. Ma, Y.Q. Zhang, K.J. Guo, Y.P. Ren, Y. Chen, J. Yang, J.Y. Qian, Variation of nanoparticles in pickering emulsions to optimize physical properties, controlled release and sustained antioxidant activity of hydroxypropyl methylcellulose-based microporous films, Int. J. Biol. Macromol. 287 (2025) 138646, https://doi.org/10.1016/j.ijbiomac.2024.138646.
[55] B. Uner, M.E. Durgun, S. Ozdemir, C. Tas, M. Uner, Y. Ozsoy, Determination of the toxicity preferences of ocular drug delivery systems by comparing two different toxicity bioassays, Assay Drug Dev. Technol. 21 (2023) 337–343, https://doi.org/10.1089/adt.2023.058.
[56] P. Budai, É. Kormos, I. Buda, G. Somody, J. Lehel, Comparative evaluation of HET-CAM and ICE methods for objective assessment of ocular irritation caused by selected pesticide products, Toxicol. Vitro 74 (2021) 105150, https://doi.org/10.1016/j.tiv.2021.105150.